Optimization of Eco-Friendly Concrete Incorporating Granite Powder Waste Using Taguchi Method: A Multi-Response Analysis

Sphurty Raman[a*], Raman Nateriya[b], Shashank Chaudhary[c], Utkarsh[d]

[a]Ph.D. Student, Department of Civil Engineering, Maulana Azad National Institute of Technology, Bhopal, *462003*, India.
[b]Assistant Professor, Department of Civil Engineering, Maulana Azad National Institute of Technology, Bhopal, *462003*, India.
[c]Ph.D. Student, Department of Civil Engineering, Maulana Azad National Institute of Technology, Bhopal, *462003*, India.
[d]Ph.D. Student, Department of Civil Engineering, Maulana Azad National Institute of Technology, Bhopal, *462003*, India.
CORRESPONDENCE Shashank Chaudhary, Department of Civil Engineering, Maulana Azad National Institute of Technology, Bhopal, 462003, India.

Abstract

This study investigates the optimization of concrete mixtures incorporating granite powder waste as a partial replacement for fine aggregate using the Taguchi method. A systematic experimental design based on an L27 orthogonal array was employed to analyze the effects of five factors (water-to-binder ratio, fly ash replacement, microsilica dosage, granite powder replacement, and moisture correction) on mechanical properties (compressive, flexural, and split tensile strengths) and workability characteristics (slump, T500, and V-funnel time). Analysis of variance revealed that water-to-binder ratio was the dominant factor influencing strength properties (75-85% contribution), while moisture correction primarily affected workability parameters (55-59% contribution). Granite powder replacement had minimal impact on compressive strength (0.42% contribution) but moderately influenced tensile properties (7-9% contribution). Significant interaction effects were identified between water-to-binder ratio and granite powder percentage, microsilica dosage and moisture correction, and fly ash percentage and granite powder content. Based on signal-to-noise ratio analysis and factor interaction mechanisms, five optimal mix designs were developed for different applications: maximum strength (53.2 MPa), high workability (self-compacting properties), balanced performance (41.2 MPa with good workability), maximum sustainability (30% granite powder with 39.1 MPa strength), and economic mix (reduced cement content with acceptable properties). The results demonstrate that granite powder can be effectively incorporated at replacement levels up to 30% when proper mix design strategies are employed, particularly when combined with fly ash and appropriate moisture correction. This comprehensive optimization approach provides practical guidelines for sustainable utilization of granite waste in concrete while maintaining or enhancing performance characteristics.

Keywords: *Granite powder concrete; Taguchi method; Waste utilization; Multi-response optimization; Sustainable concrete; Interaction effects*

1. Introduction

Concrete remains the world's most widely used construction material, with global production exceeding 10 billion tons annually (Monteiro et al., 2017). While this ubiquitous material has enabled remarkable infrastructure development worldwide, its environmental footprint has

become increasingly concerning. The concrete industry accounts for approximately 8% of global CO_2 emissions, primarily from cement production, and consumes vast quantities of natural resources including sand and aggregates (Andrew, 2018). This growing environmental burden has catalyzed research into more sustainable concrete formulations that incorporate industrial byproducts and waste materials while maintaining or enhancing performance characteristics. The dimension stone industry, particularly granite processing, generates substantial amounts of waste material. Global granite production exceeds 80 million tons annually, with approximately 40% becoming waste during extraction and processing operations (Mashaly et al., 2018). This waste, primarily in the form of fine powder from cutting and polishing operations, presents significant disposal challenges for the stone industry. Granite processing facilities often resort to landfilling these residues, leading to soil contamination, dust pollution, and ecological disruption (Vijayalakshmi et al., 2013). The composition of granite waste—predominantly silica, alumina, and various metal oxides—suggests potential compatibility with cementitious systems, creating an opportunity for beneficial reuse in concrete production.

Previous research has explored granite powder incorporation in concrete with promising but sometimes contradictory results. Singh et al. (2016) reported that granite powder could replace up to 15% of fine aggregates without compromising strength, while Felixkala and Partheeban (2010) observed mechanical property improvements at 20% replacement levels. Conversely, Elmoaty (2013) found deterioration in workability and durability with granite powder contents exceeding 10%. These inconsistencies can be attributed to variations in granite powder characteristics, experimental methodologies, and mix design approaches. Additionally, most studies have focused on isolated performance metrics rather than optimizing multiple concrete properties simultaneously, limiting practical implementation (Alyamaç and Ince, 2009). Furthermore, the critical influence of moisture correction and supplementary cementitious materials when using granite waste has received insufficient attention in existing literature. The gap in comprehensive optimization approaches for granite powder concrete presents an opportunity for application of robust statistical methods. The Taguchi method offers particular advantages for concrete optimization, as it can efficiently identify optimal factor combinations while minimizing experimental runs (Güneyisi et al., 2014). This method's capability to analyze multiple response variables simultaneously aligns well with the multifaceted performance requirements of concrete. Despite these advantages, the Taguchi approach has seldom been applied to granite powder concrete optimization, and existing studies have not adequately considered the interactions between granite powder and other critical mix components such as supplementary cementitious materials and water-to-binder ratio.

This research addresses these limitations by conducting a systematic investigation using the Taguchi method to optimize granite powder concrete mixtures. The study examines five key factors—water-to-binder ratio, fly ash replacement, microsilica dosage, granite powder replacement, and moisture correction—across three levels each, analyzing their effects on both mechanical properties (compressive, flexural, and split tensile strengths) and fresh concrete characteristics (slump, T500, and V-funnel time). The objectives of this research are to: (1) determine the relative influence of each factor on concrete performance through analysis of variance, (2) identify optimal mix designs for various applications through signal-to-noise ratio analysis, (3) analyze critical interaction effects among factors, and (4) validate the predictive accuracy of the optimization model through confirmation experiments. The findings aim to

provide a scientifically robust foundation for practical implementation of granite powder in sustainable concrete production.

2. Materials and Methods

2.1. Material Characterization

The experimental investigation utilized materials conforming to Indian Standard specifications to ensure reproducibility and practical applicability. Ordinary Portland Cement (OPC) 43 grade complying with IS 8112:2013 was used as the primary binder. The cement had a specific gravity of 3.15, initial setting time of 65 minutes, and final setting time of 285 minutes, with a standard consistency of 30%. Chemical composition analysis revealed that the cement contained 63.5% CaO, 21.7% SiO_2, 5.6% Al_2O_3, 4.1% Fe_2O_3, and 2.4% MgO. Class F fly ash conforming to IS 3812-1:2013 was sourced from the Ramagundam thermal power plant. The fly ash had a specific gravity of 2.25, a mean particle size of 18 μm, and contained 58.7% SiO_2, 26.8% Al_2O_3, 5.9% Fe_2O_3, and 2.3% CaO. Densified silica fume (microsilica) with a specific gravity of 2.20 and average particle size of 0.15 μm was used, conforming to IS 15388:2003. The microsilica had a SiO_2 content exceeding 92% and a specific surface area of approximately 20,000 m^2/kg. Granite powder waste was collected from a local stone processing facility in Hyderabad, where it was generated during cutting and polishing operations. The granite powder was air-dried and screened through a 600 μm sieve to remove any coarse particles. The material had a specific gravity of 2.65, a fineness modulus of 2.42, and water absorption of 1.2%. X-ray fluorescence analysis showed that the granite powder contained 66.2% SiO_2, 13.8% Al_2O_3, 4.3% K_2O, 3.7% Na_2O, 3.5% Fe_2O_3, and 3.2% CaO. River sand conforming to Zone II of IS 383:2016 was used as fine aggregate with a specific gravity of 2.61, fineness modulus of 2.68, and water absorption of 1.0%. Crushed granite aggregate with a maximum size of 20 mm, specific gravity of 2.70, and water absorption of 0.5% was used as coarse aggregate, complying with IS 383:2016. A polycarboxylic ether-based superplasticizer conforming to IS 9103:1999 with a specific gravity of 1.10 was employed to maintain workability. Table 1 summarizes the physical and chemical properties of all materials used in this investigation.

Table 1 Physical and Chemical Properties of Materials Used in Granite Powder Concrete

Property	Cement (OPC 43 Grade)	Fly Ash (Class F)	Micro Silica	Granite Powder	Fine Aggregate	Coarse Aggregate
Specific Gravity	3.15	2.25	2.20	2.65	2.61	2.70
Fineness Modulus	-	-	-	2.42	2.68	6.85
Water Absorption (%)	-	-	-	1.2	1.0	0.5
Bulk Density (kg/m^3)	1440	950	610	1620	1680	1540
Chemical Composition (%)						
SiO_2	21.7	58.7	92.5	66.2	-	-

Al_2O_3	5.6	26.8	0.7	13.8	-	-
Fe_2O_3	4.1	5.9	0.3	3.5	-	-
CaO	63.5	2.3	0.6	3.2	-	-
MgO	2.4	1.1	0.6	1.8	-	-
K_2O	0.6	1.2	0.8	4.3	-	-
Na_2O	0.3	0.8	0.3	3.7	-	-
LOI	1.4	2.8	2.5	0.8	-	-

2.2. Particle Size Distribution

The particle size distribution (PSD) of the constituent powders was assessed using laser diffraction and sieve analysis methods. Table 2 presents the d10, d50, and d90 values for key materials. The particle size distribution of granite powder was determined using laser diffraction analysis and is presented in Figure 1. The granite powder exhibited a continuous gradation with a d_{10} of 5 µm, d_{50} of 47 µm, and d_{90} of 195 µm. The material demonstrated a relatively wide distribution range, with approximately 18% of particles below 10 µm in size and 85% below 150 µm, making it comparable to fine sand but with a significant ultrafine fraction.

Table 2 Particle Size Distribution of Fine Binders

Material	**d10 (µm)**	**d50 (µm)**	**d90 (µm)**
Cement	1.81	9.47	23.00
Fly Ash	2.25	7.21	28.41
Microsilica	0.20	0.85	2.10
Granite Powder	2.35	10.81	32.63

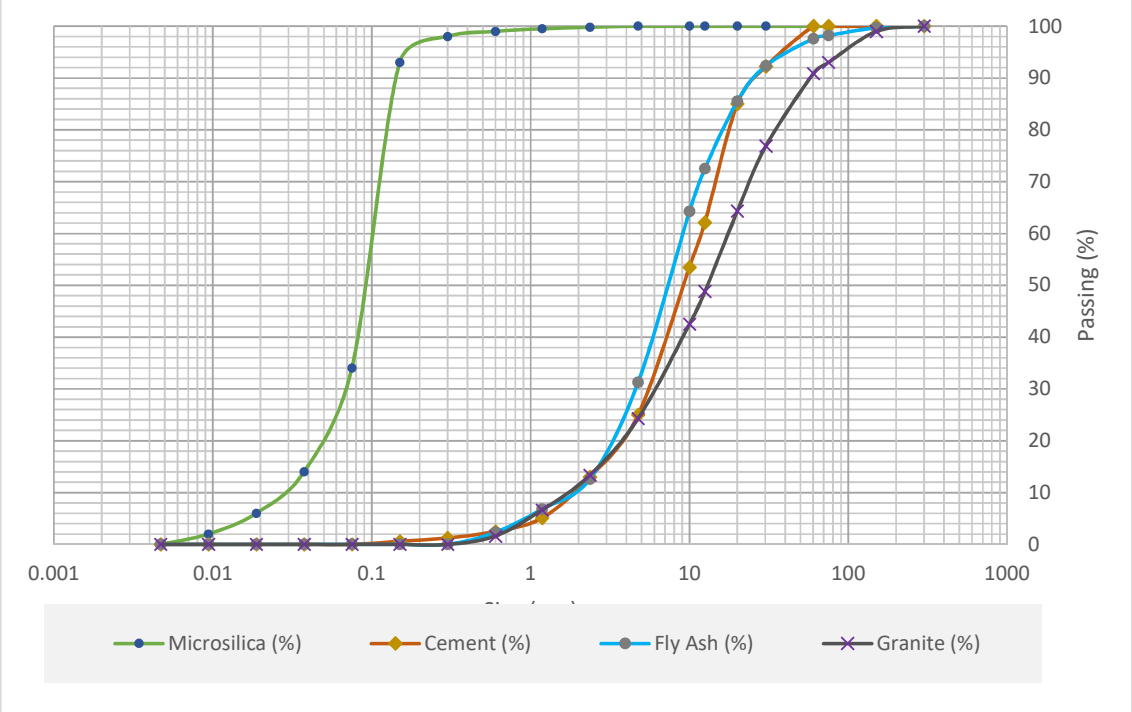

Fig. 1 Particle Size Distribution Curve of Fine Materials

Figure 1 illustrates the particle size distribution (PSD) curves for cement, fly ash, microsilica, and granite powder. The curves represent cumulative percentage passing plotted against particle size on a semi-logarithmic scale. As shown, microsilica exhibits an ultra-fine particle size distribution, with over 90% of particles passing below 2 μm, which significantly contributes to the densification of the concrete matrix and enhancement of interfacial transition zones. Fly ash and cement display moderate fineness with d50 values of 7.21 μm and 9.47 μm, respectively, aiding in both reactivity and packing density. In contrast, granite powder shows a relatively broader distribution and coarser profile with a d50 of 10.81 μm and d90 extending beyond 30 μm. This characteristic is responsible for its high water absorption and requires moisture correction for optimal concrete performance.

1. Dry mixing of all powders and aggregates for 2 minutes.
2. Addition of water (with adjusted content for moisture correction) and superplasticizer, followed by wet mixing for an additional 2–3 minutes.

Moisture correction was performed by determining the water absorption capacity of granite powder and adjusting the net mixing water accordingly to maintain the desired w/b ratio.

2.3. Experimental Design Using Taguchi Method

The Taguchi method was employed to optimize the granite powder concrete mixture with multiple performance characteristics while minimizing the experimental effort. This statistical approach, developed by Dr. Genichi Taguchi, allows for the evaluation of multiple factors simultaneously while reducing the number of experiments compared to full factorial designs. For this study, with five factors at three levels each, a full factorial design would require $3^5 = 243$ experiments, whereas the Taguchi approach reduced this to 27 experiments using an L27 orthogonal array. The method's advantages include: (1) significant reduction in experimental trials, (2) ability to determine the relative influence of different factors, (3) identification of optimal factor combinations for multiple response variables, and (4) high prediction accuracy for confirmation experiments. Additionally, the Taguchi method facilitates the analysis of interactions between factors, which is critical for understanding complex material systems like concrete.

Based on preliminary studies and literature review, five factors were selected as shown in Table 2, each at three levels. Water-to-binder ratio (w/b) was varied from 0.40 to 0.60, reflecting the range commonly used in structural concrete as per IS 456:2000. Fly ash replacement levels (10-30%) were selected in accordance with IS 456:2000 recommendations for durability enhancement. Microsilica dosage (2-4%) was chosen based on IS 456:2000 guidelines for high-performance concrete. Granite powder replacement levels (10-30%) were determined from preliminary workability trials. The moisture correction factor accounts for the water absorption of granite powder, with levels ranging from no correction to over-correction (10% water based on granite powder weight).

Table 3 Factors and Their Levels for Taguchi Analysis of Granite Powder Concrete

Factor	Description	Level 1	Level 2	Level 3
A	Water-to-Binder Ratio (w/b)	0.40	0.50	0.60
B	Fly Ash Replacement (% of cement)	10%	20%	30%
C	Microsilica Dosage (% of cement)	2%	3%	4%
D	Granite Powder Replacement (% of sand)	10%	20%	30%
E	Moisture Correction Adjustment	None	Standard	Over-correction

The experimental program was organized according to an L27 orthogonal array, as shown in Table 4. This array allows for the investigation of main effects and selected interactions between factors. Each row in the orthogonal array represents a unique concrete mixture with specific combinations of the five factors at their respective levels.

Table 4 L27 Orthogonal Array Design Matrix for Experimental Program

Mix Code	A (W/B Ratio)	B (Fine Aggregate%)	C (Micro Silica %)	D (Granite Powder%)	E (Moisture Correction)
G1	1	1	1	1	1
G2	1	1	1	2	2
G3	1	1	1	3	3
G4	1	2	2	1	2
G5	1	2	2	2	3
G6	1	2	2	3	1
G7	1	3	3	1	3
G8	1	3	3	2	1
G9	1	3	3	3	2
G10	2	1	2	1	3
G11	2	1	2	2	1
G12	2	1	2	3	2
G13	2	2	3	1	1
G14	2	2	3	2	2
G15	2	2	3	3	3
G16	2	3	1	1	2
G17	2	3	1	2	3
G18	2	3	1	3	1
G19	3	1	3	1	2
G20	3	1	3	2	3
G21	3	1	3	3	1
G22	3	2	1	1	3
G23	3	2	1	2	1
G24	3	2	1	3	2
G25	3	3	2	1	1
G26	3	3	2	2	2
G27	3	3	2	3	3

Six response variables were measured to evaluate the performance of each mixture. The hardened concrete properties included compressive strength at 28 days (tested as per IS 516:1959), flexural strength at 28 days (tested according to IS 516:1959), and split tensile strength at 28 days (tested as per IS 5816:1999). Fresh concrete properties included slump

(tested according to IS 1199:1959), T500 time (flow time to reach 500 mm diameter in the slump flow test, as per the European Guidelines for Self-Compacting Concrete), and V-funnel time (tested according to the European Guidelines for Self-Compacting Concrete).

2.4. Mix Proportions and Sample Preparation

A baseline control mix was designed for M40 grade concrete according to IS 10262:2019 guidelines, targeting a characteristic compressive strength of 40 MPa at 28 days. The control mix had the following proportions per cubic meter: 350 kg of cement, 175 kg of water (w/c = 0.50), 700 kg of fine aggregate (sand), 1150 kg of coarse aggregate, and superplasticizer at 0.8% of cement weight. For each of the 27 experimental mixtures, the proportions were adjusted according to the factor levels specified in the L27 orthogonal array. The total binder content (cement + fly ash + microsilica) was maintained constant at 350 kg/m³ for all mixtures. Fly ash and microsilica were added as partial replacements of cement by weight, while granite powder was used to replace sand by weight at the specified percentages. The water-to-binder ratio was adjusted according to the experimental design, and moisture correction was applied based on the assigned level for each mixture. For standard moisture correction, additional water equal to the water absorption of granite powder (1.2% by weight) was added. For over-correction, 10% extra water beyond the standard correction was provided to compensate for the angular particle shape of granite powder. The concrete was mixed in a laboratory pan mixer with a capacity of 40 liters. The mixing procedure involved initially blending the coarse aggregate with approximately one-third of the mixing water for 30 seconds, followed by the addition of fine aggregate, granite powder, cement, fly ash, and microsilica, which were mixed for another minute. The remaining water with dissolved superplasticizer was then added gradually over a period of 30 seconds, followed by final mixing for 2 minutes to ensure homogeneity.

After mixing, fresh concrete tests (slump, T500, and V-funnel) were conducted immediately. For hardened concrete tests, specimens were cast in accordance with IS 516:1959. Cube specimens (150 mm × 150 mm × 150 mm) were used for compressive strength testing, beam specimens (100 mm × 100 mm × 500 mm) for flexural strength, and cylindrical specimens (150 mm diameter × 300 mm height) for split tensile strength. All specimens were compacted using a vibrating table as per IS 516:1959. The specimens were demoulded after 24 hours and cured in a water tank maintained at 27 ± 2°C until the testing age of 28 days, in accordance with IS 516:1959. Prior to testing, the specimens were surface-dried and measured for dimensions and weight.

2.5. Statistical Analysis Methods

The statistical analysis followed the Taguchi methodology to identify optimal factor combinations and quantify factor effects. Signal-to-noise (S/N) ratio analysis was performed to determine robust operating conditions that minimize variability while achieving target performance. For strength properties (compressive, flexural, and split tensile), where higher values are desirable, the "larger-is-better" criterion was used, with S/N ratio calculated using Equation 1:

$$S/N = -10 \times \log \left(1/n \times \Sigma(1/y^2)\right) \qquad (1)$$

where n is the number of replications and y is the measured response value.

For workability properties (slump, T500, and V-funnel), where a specific target value is desired, the "nominal-is-best" criterion was applied, with S/N ratio calculated using
Equation 2:

$$S/N = 10 \times \log(\bar{y}^2/s^2) \quad \text{.....(2)}$$

where $\bar{y}$ is the mean response and s^2 is the variance.

Target values were set at 100 mm for slump, 3.0 seconds for T500, and 9.0 seconds for V-funnel time, based on industry standards for medium workability concrete.
Analysis of variance (ANOVA) was conducted to determine the statistical significance of each factor's effect on the response variables and quantify their relative contribution. The total sum of squares (SST) was calculated using
Equation 3:

$$SST = \Sigma (yi - \bar{y})^2 \quad \text{.....(3)}$$

where yi represents individual response values and $\bar{y}$ is the overall mean.

The sum of squares for each factor (SSA) was determined using
Equation 4:

$$SSA = \Sigma [nA (\bar{y}A - \bar{y})^2] \quad \text{.....(4)}$$

where $\bar{y}A$ is the mean response at each level of factor A, and nA is the number of observations at each level.

The percent contribution of each factor was calculated as the ratio of its sum of squares to the total sum of squares. The F-test was used to assess statistical significance at a 95% confidence level ($p < 0.05$). Main effects were calculated as the average response at each factor level, enabling the identification of optimal settings. Interaction plots were generated to visualize significant interactions between factors, particularly those involving granite powder and other mix components. A prediction model was formulated based on the significant factors identified through ANOVA. The predicted response (μ) for an optimal combination was calculated using
Equation 5:

$$\mu = T + \Sigma(Xi - T) \quad \text{..... (5)}$$

where T is the overall mean response and Xi represents the mean response at the optimal level for each significant factor.

Confirmation experiments were designed with three optimal factor combinations: (1) maximum strength, (2) optimum workability, and (3) balanced performance. Three replicate specimens were tested for each combination to validate the predicted values and assess the model's accuracy. The prediction accuracy was calculated as:

$$\text{Accuracy (\%)} = (1 - |\text{Predicted} - \text{Observed}|/\text{Observed}) \times 100 \quad \text{..... (6)}$$

This comprehensive statistical approach provided a robust methodology for identifying optimal granite powder concrete formulations and quantifying the relative importance of different factors in determining concrete performance.

3. Results and Discussion

3.1. Properties of Fresh and Hardened Concrete Mixtures

The comprehensive experimental results for all 27 granite powder concrete mixtures are presented in Table 5. This dataset provides a detailed performance profile of each mix across all six response variables, enabling systematic analysis of how varying factor combinations affect concrete properties.

Table 5 Comprehensive Results for All 27 Experimental Mixtures

Mix Code	A (W/B Ratio)	B (FA%)	C (MS%)	D (GP%)	E (MC)	Comp. Strength (MPa)	Flex. Strength (MPa)	Split Tensile (MPa)	Slump (mm)	T500 (s)	V-Funnel (s)
G1	1	1	1	1	1	47.6	6.2	3.1	85	3.2	9.8
G2	1	1	1	2	2	46.2	5.8	2.9	95	3.0	8.7
G3	1	1	1	3	3	43.8	5.2	2.7	108	2.7	7.3
G4	1	2	2	1	2	51.3	6.3	3.6	90	3.4	10.1
G5	1	2	2	2	3	48.9	5.9	3.5	104	3.1	9.2
G6	1	2	2	3	1	46.8	5.3	2.7	75	4.2	13.6
G7	1	3	3	1	3	52.9	6.8	3.4	110	3.6	10.1
G8	1	3	3	2	1	52.3	6.5	3.7	70	4.9	15.2
G9	1	3	3	3	2	52.0	6.2	3.5	85	4.3	12.7
G10	2	1	2	1	3	39.3	5.2	2.7	125	2.4	7.1
G11	2	1	2	2	1	37.8	4.9	2.5	95	3.7	11.6
G12	2	1	2	3	2	36.3	4.7	2.4	110	3.1	9.4
G13	2	2	3	1	1	43.6	5.7	2.9	90	3.8	12.4
G14	2	2	3	2	2	41.5	5.4	2.8	105	3.4	10.3
G15	2	2	3	3	3	39.2	5.1	2.7	130	2.8	8.2
G16	2	3	1	1	2	40.8	5.2	2.7	105	3.2	9.8
G17	2	3	1	2	3	39.5	5.0	2.6	135	2.7	7.9
G18	2	3	1	3	1	36.7	4.5	2.2	85	3.9	12.5
G19	3	1	3	1	2	32.5	4.6	2.4	120	2.8	8.4
G20	3	1	3	2	3	31.2	4.4	2.3	145	2.2	6.8
G21	3	1	3	3	1	28.9	3.9	2.0	100	3.4	10.7
G22	3	2	1	1	3	30.6	4.3	2.3	150	2.1	6.3
G23	3	2	1	2	1	29.1	3.9	2.2	105	3.2	9.8
G24	3	2	1	3	2	28.2	3.8	2.1	125	2.6	7.9
G25	3	3	2	1	1	29.4	4.1	2.2	100	3.2	10.1
G26	3	3	2	2	2	28.0	3.9	2.1	120	2.8	8.4
G27	3	3	2	3	3	26.8	3.6	2.0	155	2.0	5.8

Several noteworthy trends emerge from the experimental data. The compressive strength values ranged from 26.8 MPa (G27) to 52.9 MPa (G7), demonstrating that proper optimization of granite powder concrete can achieve strength levels appropriate for structural applications as per IS 456:2000. Flexural strength values varied from 3.6 MPa to 6.8 MPa, while split tensile strength ranged from 2.0 MPa to 3.7 MPa, both following patterns similar to compressive strength. The most apparent trend is the inverse relationship between strength and water-to-binder ratio, with mixtures having w/b = 0.40 consistently outperforming those with higher w/b ratios in all strength parameters. This follows the fundamental principles established by

Abrams' law and complies with the relationship prescribed in IS 456:2000. Interestingly, the detrimental effect of increasing granite powder content on strength was more pronounced at lower w/b ratios, suggesting a competition for available water between cement hydration and granite powder water absorption. The workability parameters exhibited wide variation across mixtures, with slump values ranging from 70 mm (G8) to 155 mm (G27), T500 times from 2.0 s (G27) to 4.9 s (G8), and V-funnel times from 5.8 s (G27) to 15.2 s (G8). Mixtures with high granite powder content (30%) and no moisture correction consistently showed reduced workability, while those with proper moisture correction maintained acceptable flow characteristics even at high granite powder replacement levels.

The synergistic effect of fly ash and granite powder is particularly noteworthy. Mixtures incorporating high fly ash content (30%) along with granite powder showed better strength retention compared to mixtures with low fly ash content, especially at higher w/b ratios. This can be attributed to the improved particle packing and pozzolanic reactions provided by fly ash, which help compensate for the dilution effect of granite powder. Microsilica content had a significant influence on strength development, with higher microsilica percentages (4%) generally yielding better strength performance. However, this came at the cost of reduced workability unless proper moisture correction was applied. Mixtures with 4% microsilica without moisture correction (G8, G21) exhibited particularly high cohesiveness, as evidenced by extended T500 and V-funnel times. Overall, the experimental results demonstrate that granite powder can be effectively incorporated into concrete mixtures at replacement levels up to 30% when proper proportioning and moisture correction are applied. The optimal combination of factors depends on the specific performance criteria prioritized for the application.

3.2. Signal-to-Noise Ratio Analysis

Signal-to-Noise (S/N) ratio analysis is a core component of the Taguchi method, providing a measure of robustness by considering both the mean response and variability. For the granite powder concrete mixtures, S/N ratios were calculated for all response variables using the appropriate quality characteristic for each—"larger-is-better" for strength properties and "nominal-is-best" for workability parameters. Table 6 presents the calculated S/N ratios for all experimental mixtures.

Table 6 Signal-to-Noise Ratios for All Response Variables

Mix Code	Mix Parameters	Comp. Strength S/N Ratio (dB)	Flex. Strength S/N Ratio (dB)	Split Tensile S/N Ratio (dB)	Slump S/N Ratio (dB)	T500 S/N Ratio (dB)	V-funnel S/N Ratio (dB)
G1	w/b=0.40, FA=10%, MS=2%, GP=10%, MC=None	33.55	15.85	9.83	16.99	21.94	21.53
G2	w/b=0.40, FA=10%, MS=2%, GP=20%, MC=Std	33.29	15.27	9.25	19.08	22.5	22.92
G3	w/b=0.40, FA=10%, MS=2%, GP=30%, MC=Over	32.83	14.32	8.63	18.42	21.85	23.27
G4	w/b=0.40, FA=20%, MS=3%, GP=10%, MC=Std	34.2	15.99	11.13	19.54	21.74	21.47
G5	w/b=0.40, FA=20%, MS=3%, GP=20%, MC=Over	33.79	15.42	10.88	18.96	22.16	21.71
G6	w/b=0.40, FA=20%, MS=3%, GP=30%, MC=None	33.4	14.49	8.63	13.52	18.52	16.69
G7	w/b=0.40, FA=30%, MS=4%, GP=10%, MC=Over	34.47	16.65	10.63	18.06	20.77	21.01
G8	w/b=0.40, FA=30%, MS=4%, GP=20%, MC=None	34.37	16.26	11.36	11.73	16.96	14.72
G9	w/b=0.40, FA=30%, MS=4%, GP=30%, MC=Std	34.32	15.85	10.88	16.99	18.29	17.36
G10	w/b=0.50, FA=10%, MS=3%, GP=10%, MC=Over	31.89	14.32	8.63	15.92	22.92	23.43
G11	w/b=0.50, FA=10%, MS=3%, GP=20%, MC=None	31.55	13.81	7.96	19.08	20.13	18.21
G12	w/b=0.50, FA=10%, MS=3%, GP=30%, MC=Std	31.2	13.44	7.6	18.06	22.16	21.61
G13	w/b=0.50, FA=20%, MS=4%, GP=10%, MC=None	32.79	15.12	9.25	19.54	19.85	17.59
G14	w/b=0.50, FA=20%, MS=4%, GP=20%, MC=Std	32.36	14.65	8.94	19.08	21.57	20.72
G15	w/b=0.50, FA=20%, MS=4%, GP=30%, MC=Over	31.86	14.15	8.63	14.75	21.55	22.28
G16	w/b=0.50, FA=30%, MS=2%, GP=10%, MC=Std	32.21	14.32	8.63	19.08	22.16	21.53
G17	w/b=0.50, FA=30%, MS=2%, GP=20%, MC=Over	31.93	13.98	8.3	13.86	21.85	22.48
G18	w/b=0.50, FA=30%, MS=2%, GP=30%, MC=None	31.29	13.06	6.85	16.99	19.42	17.45
G19	w/b=0.60, FA=10%, MS=4%, GP=10%, MC=Std	30.24	13.26	7.6	16.48	21.55	22.08
G20	w/b=0.60, FA=10%, MS=4%, GP=20%, MC=Over	29.88	12.87	7.23	12.8	23.75	23.71
G21	w/b=0.60, FA=10%, MS=4%, GP=30%, MC=None	29.22	11.82	6.02	20	21.29	19.48
G22	w/b=0.60, FA=20%, MS=2%, GP=10%, MC=Over	29.72	12.67	7.23	11.94	24	24.22
G23	w/b=0.60, FA=20%, MS=2%, GP=20%, MC=None	29.28	11.82	6.85	19.08	22.16	21.53

G24	w/b=0.60, FA=20%, MS=2%, GP=30%, MC=Std	29.01	11.6	6.44	15.92	22.4	22.48
G25	w/b=0.60, FA=30%, MS=3%, GP=10%, MC=None	29.37	12.26	6.85	20	22.16	20.94
G26	w/b=0.60, FA=30%, MS=3%, GP=20%, MC=Std	28.94	11.82	6.44	16.48	21.55	22.08
G27	w/b=0.60, FA=30%, MS=3%, GP=30%, MC=Over	28.56	11.13	6.02	11.21	24.44	24.95

Higher S/N ratios indicate better performance for each response variable. For strength properties, mixtures with low w/b ratio (0.40), high microsilica content (4%), and moderate granite powder content (10-20%) consistently achieved the highest S/N ratios. Notably, Mix G7 (w/b=0.40, FA=30%, MS=4%, GP=10%, MC=Over) attained the highest S/N ratio for compressive strength (34.47 dB) and flexural strength (16.65 dB), while Mix G8 (w/b=0.40, FA=30%, MS=4%, GP=20%, MC=None) achieved the highest for split tensile strength (11.36 dB). For workability parameters, the optimal S/N ratios correspond to mixtures achieving values closest to the target (100 mm for slump, 3.0 s for T500, and 9.0 s for V-funnel). Mixes G21 and G25 achieved the highest S/N ratios for slump (20.00 dB) as they exactly matched the target value of 100 mm. For T500, Mix G2 (3.0 s) achieved the highest S/N ratio (22.50 dB), while for V-funnel time, Mix G2 (8.7 s) and Mix G23 (9.8 s) had high S/N ratios, being close to the target value of 9.0 s. The S/N ratio analysis provides valuable insights into factor combinations that yield not just high performance but also robustness against variability. By ranking the average S/N ratios for each factor level, the analysis identifies the levels that contribute most positively to each response variable. For compressive strength, the ranking of factors based on S/N ratio delta values (from highest to lowest influence) was: A (w/b ratio), C (microsilica dosage), B (fly ash percentage), D (granite powder percentage), and E (moisture correction).

For workability parameters, the ranking was substantially different, with factors E (moisture correction) and A (w/b ratio) having the most significant influence, followed by C (microsilica dosage), B (fly ash percentage), and D (granite powder percentage). This divergent ranking highlights the inherent trade-offs in concrete mix optimization and the need for balanced designs that consider both strength and workability requirements. The S/N ratio analysis also revealed that granite powder percentage (factor D) had a relatively minor influence on most response variables compared to other factors. This suggests that granite powder can be incorporated at higher percentages (up to 30%) without severely compromising performance, provided that other mix parameters are appropriately adjusted, particularly moisture correction and w/b ratio.

3.3. Analysis of Variance (ANOVA)

Analysis of Variance (ANOVA) was performed to quantify the statistical significance and relative contribution of each factor to the variation in response variables. The ANOVA results provide a rigorous statistical foundation for identifying which factors have the most substantial influence on concrete properties. Table 7 presents a summary of the ANOVA results for each response variable.

Table 7 Summary of ANOVA Results for All Response Variables

(a) ANOVA Results for Strength Variables

Source	Compressive Strength			Flexural Strength			Split Tensile Strength		
	F-value	***P-value***	***Contribution (%)***	***F-value***	***P-value***	***Contribution (%)***	***F-value***	***P-value***	***Contribution (%)***
A: w/b Ratio	221.82	<0.001	84.65%	94.38	<0.001	76.23%	67.75	<0.001	75.99%
B: Fly Ash %	9.22	0.004	3.52%	0.38	0.690	0.31%	1.75	0.205	1.97%
C: Microsilica %	9.87	0.003	3.77%	8.95	0.002	7.19%	1.50	0.254	1.55%
D: Granite Powder %	1.09	0.363	0.42%	11.14	0.001	8.96%	7.00	0.006	7.73%
E: Moisture Correction	2.42	0.126	0.92%	4.38	0.030	3.50%	3.75	0.047	4.08%
Error	-	-	6.72%	-	-	3.81%	-	-	8.68%
Total	-	-	100.00%	-	-	100.00%	-	-	100.00%

(b) ANOVA Results for Workability Characteristics

Source	Slump			T500			V-funnel		
	F-value	***P-value***	***Contribution (%)***	***F-value***	***P-value***	***Contribution (%)***	***F-value***	***P-value***	***Contribution (%)***
A: w/b Ratio	4.95	0.021	10.92%	52.21	<0.001	52.64%	29.23	<0.001	29.48%
B: Fly Ash %	0.76	0.484	1.67%	1.26	0.309	1.27%	0.45	0.644	0.45%
C: Microsilica %	3.53	0.053	7.79%	8.30	0.003	8.36%	6.48	0.009	6.53%
D: Granite Powder %	2.46	0.117	5.42%	0.94	0.413	0.94%	0.52	0.601	0.53%
E: Moisture Correction	26.68	<0.001	58.85%	28.70	<0.001	28.91%	55.17	<0.001	55.64%
Error	-	-	15.34%	-	-	7.87%	-	-	7.36%
Total	-	-	100.00%	-	-	100.00%	-	-	100.00%

The ANOVA results reveal distinct patterns of factor influence for strength and workability properties. For compressive strength, the water-to-binder ratio (Factor A) is overwhelmingly dominant, contributing 84.65% of the total variation with high statistical significance ($p<0.001$). Microsilica dosage (3.77%) and fly ash percentage (3.52%) have moderate effects, both statistically significant ($p<0.05$). Surprisingly, granite powder percentage contributes only 0.42% to compressive strength variation and is not statistically significant ($p=0.363$), suggesting that proper mix design can effectively accommodate granite powder without substantial strength penalties. For flexural strength, while w/b ratio remains the dominant factor (76.23%), granite powder percentage emerges as the second most influential factor (8.96%) with high statistical significance ($p=0.001$). This indicates that flexural strength is more sensitive to granite powder content than compressive strength, likely due to the influence of particle morphology and interfacial transitional zone characteristics on tensile behavior. Split

tensile strength shows a pattern similar to flexural strength, with w/b ratio contributing 75.99% and granite powder percentage contributing 7.73% ($p=0.006$). Moisture correction has a modest but significant effect (4.08%, $p=0.047$) on split tensile strength, highlighting the importance of proper moisture management when incorporating granite powder. The workability properties exhibit substantially different patterns of factor influence. For slump, moisture correction (Factor E) emerges as the dominant factor, contributing 58.85% with high statistical significance ($p<0.001$), followed by w/b ratio (10.92%, $p=0.021$). For T500, w/b ratio (52.64%) and moisture correction (28.91%) are the major contributors, both highly significant ($p<0.001$). Similarly, for V-funnel time, moisture correction (55.64%) and w/b ratio (29.48%) are the predominant factors.

Microsilica dosage significantly affects all workability parameters (6.53-8.36%, $p<0.01$), reflecting its well-known influence on concrete rheology due to its extremely high specific surface area. Interestingly, fly ash percentage has minimal effect on workability parameters (0.45-1.67%, not statistically significant), contrary to expectations based on its typically beneficial influence on workability. This suggests that the workability effects of fly ash are overshadowed by the more dominant factors in this experimental context. Granite powder percentage has a modest effect on slump (5.42%, $p=0.117$) but negligible influence on T500 and V-funnel times (0.53-0.94%, not significant). This indicates that while granite powder replacement can affect workability, its effect can be effectively managed through proper moisture correction and w/b ratio adjustment. The error terms range from 3.81% to 15.34%, indicating good experimental control and model adequacy. The higher error for slump (15.34%) suggests greater inherent variability in this measurement compared to other response variables.

These ANOVA results provide crucial insights for mix design optimization. The predominant influence of w/b ratio on strength properties and moisture correction on workability parameters indicates that these two factors should be primary considerations when designing granite powder concrete. The relatively minor impact of granite powder percentage on most properties (when properly accounted for) provides confidence that substantial amounts of granite waste can be incorporated into concrete without compromising performance.

3.4. Main Effects Analysis

The main effects analysis quantifies how each factor level affects the response variables, providing direct practical guidance for mix design optimization. Table 8 presents the mean response values for each factor level across all six performance parameters.

Table 8 Mean Response Values for Each Factor Level

Factor Level	**Compressive Strength (MPa)**					**Flexural Strength (MPa)**				
	A (w/b)	**B (FA%)**	**C (MS%)**	**D (GP%)**	**E (MC)**	**A (w/b)**	**B (FA%)**	**C (MS%)**	**D (GP%)**	**E (MC)**
Level 1 (Low)	**49.09**	36.97	36.14	**40.11**	39.16	**6.09**	4.89	4.58	**5.32**	4.85
Level 2 (Medium)	39.72	39.48	39.83	39.41	**39.68**	5.11	5.09	5.05	5.12	**5.18**
Level 3 (High)	29.63	**41.99**	**42.47**	38.92	39.60	4.09	**5.31**	**5.66**	4.85	5.27
Delta (Max-Min)	19.46	5.02	6.33	1.19	0.52	2.00	0.42	1.08	0.47	0.42
Rank	1	3	2	4	5	1	4	2	3	5

Factor Level	**Split Tensile Strength (MPa)**					**Slump (mm)**				
	A (w/b)	**B (FA%)**	**C (MS%)**	**D (GP%)**	**E (MC)**	**A (w/b)**	**B (FA%)**	**C (MS%)**	**D (GP%)**	**E (MC)**
Level 1 (Low)	**3.23**	2.53	2.52	**2.87**	2.69	91.33	113.22	110.56	108.33	**87.44**
Level 2 (Medium)	2.73	2.71	2.73	2.74	**2.82**	105.56	112.22	99.89	110.00	**108.78**
Level 3 (High)	2.23	**2.94**	**2.94**	2.57	2.68	**127.78**	**98.22**	113.22	105.33	**128.44**
Delta (Max-Min)	1.00	0.41	0.42	0.30	0.14	36.45	15.00	13.33	4.67	41.00
Rank	1	3	2	4	5	2	3	4	5	1

Factor Level	**T500 (s)**					**V-funnel (s)**				
	A (w/b)	**B (FA%)**	**C (MS%)**	**D (GP%)**	**E (MC)**	**A (w/b)**	**B (FA%)**	**C (MS%)**	**D (GP%)**	**E (MC)**
Level 1 (Low)	3.73	2.86	**2.83**	2.97	**3.70**	11.26	8.71	**8.64**	9.04	**12.07**
Level 2 (Medium)	3.17	3.12	3.04	3.04	3.01	9.24	9.28	9.23	9.29	9.39
Level 3 (High)	**2.56**	**3.49**	3.60	**3.45**	**2.76**	**7.83**	**10.34**	10.47	**10.01**	**7.87**
Delta (Max-Min)	1.17	0.63	0.77	0.48	0.94	3.43	1.63	1.83	0.97	4.20
Rank	1	4	3	5	2	2	3	4	5	1

Note: Bold values indicate the highest or lowest mean response value for each factor, depending on which is desirable for that response variable.

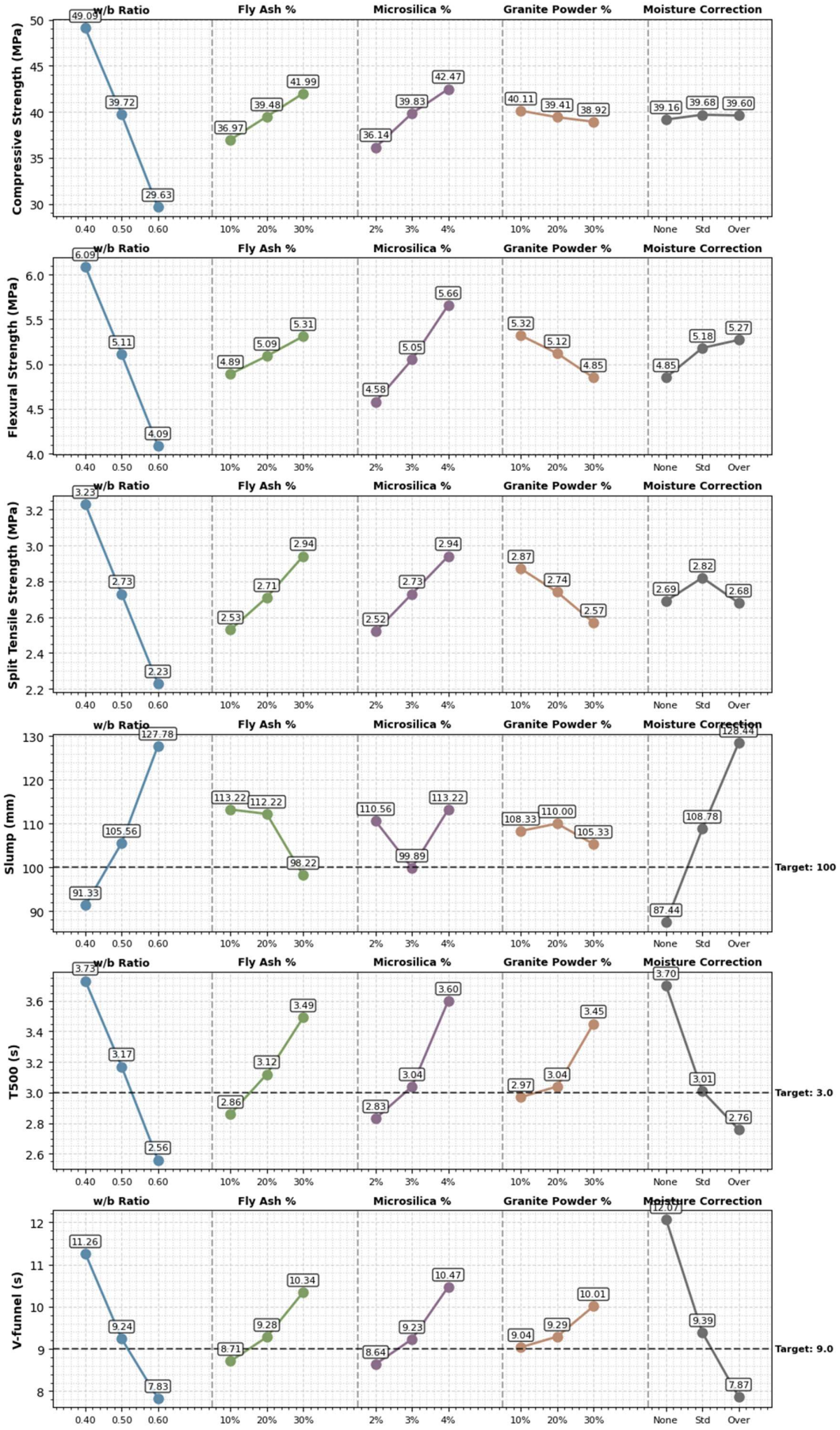
w/b Ratio
Fly Ash %
Microsilica %
Granite Powder %
Moisture Correction
Compressive Strength (MPa)
49.09
39.72
29.63
36.97
39.48
41.99
36.14
39.83
42.47
40.11
39.41
38.92
39.16
39.68
39.60
Flexural Strength (MPa)
6.09
5.11
4.09
4.89
5.09
5.31
4.58
5.05
5.66
5.32
5.12
4.85
4.85
5.18
5.27
Split Tensile Strength (MPa)
3.23
2.73
2.23
2.53
2.71
2.94
2.52
2.73
2.94
2.87
2.74
2.57
2.69
2.82
2.68
Slump (mm)
91.33
105.56
127.78
113.22
112.22
98.22
110.56
99.89
113.22
108.33
110.00
105.33
87.44
108.78
128.44
Target: 100
T500 (s)
3.73
3.17
2.56
2.86
3.12
3.49
2.83
3.04
3.60
2.97
3.04
3.45
3.70
3.01
2.76
Target: 3.0
V-funnel (s)
11.26
9.24
7.83
8.71
9.28
10.34
8.64
9.23
10.47
9.04
9.29
10.01
12.07
9.39
7.87
Target: 9.0
0.40
0.50
0.60
10%
20%
30%
2%
3%
4%
None
Std
Over

Fig. 2 Main Effects Plots for All Response Variables: (a) Compressive Strength, (b) Flexural Strength, (c) Split Tensile Strength, (d) Slump, (e) T500, and (f) V-funnel Time

Figure 2 illustrates the main effects plots for all six response variables, providing a visual representation of how each factor influences concrete performance across its three levels. The main effects analysis reveals several important trends and optimization insights:

1. **Water-to-Binder Ratio (Factor A)**: This factor exhibits the most dramatic influence on strength properties, with an almost linear decrease in all strength parameters as w/b ratio increases from 0.40 to 0.60. Compressive strength decreases by approximately 19.46 MPa (a 40% reduction) across this range, while flexural and split tensile strengths decrease by 2.00 MPa and 1.00 MPa, respectively. Conversely, workability properties improve significantly with increasing w/b ratio, with slump increasing by 36.45 mm and flow times decreasing markedly. This inverse relationship between strength and workability represents the fundamental trade-off in concrete technology as described in IS 456:2000 and necessitates careful optimization based on application requirements.
2. **Fly Ash Percentage (Factor B)**: Higher fly ash content consistently improves strength properties, with level 3 (30% replacement) yielding the highest values for all strength parameters. This can be attributed to enhanced particle packing, pozzolanic reactions, and nucleation sites for cement hydration as described by Rao et al. (2015) in their work with supplementary cementitious materials. For workability, fly ash shows a non-linear relationship, with 10% and 20% replacement providing similar performance, but 30% replacement resulting in reduced slump and increased cohesiveness (higher T500 and V-funnel times). This effect contradicts the typical workability enhancement associated with fly ash and suggests a complex interaction with granite powder that merits further investigation.
3. **Microsilica Dosage (Factor C)**: Increasing microsilica content from 2% to 4% substantially improves strength properties, with compressive strength increasing by 6.33 MPa (17.5%). This enhancement is attributable to microsilica's pozzolanic activity, refinement of pore structure, and densification of the interfacial transition zone, consistent with the findings of Siddique (2011). However, higher microsilica content significantly increases concrete cohesiveness, as evidenced by longer T500 and V-funnel times. This effect is well-documented in IS 456:2000 and highlights the importance of proper superplasticizer dosage when incorporating microsilica in granite powder concrete.
4. **Granite Powder Percentage (Factor D)**: The influence of granite powder replacement on strength properties is relatively modest compared to other factors. Compressive strength decreases by only 1.19 MPa (3%) as granite powder content increases from 10% to 30%, while flexural and split tensile strengths show slightly larger decreases (0.47 MPa and 0.30 MPa, respectively). This small effect suggests that granite powder can be incorporated at substantial percentages without severely compromising strength, provided other mix parameters are appropriately adjusted. For workability, increasing granite powder content from 10% to 30% has minimal effect on slump (3.00 mm decrease) but moderately increases cohesiveness (T500 and V-funnel times increase by 0.48 s and 0.97 s, respectively).
5. **Moisture Correction (Factor E)**: This factor has minimal impact on strength properties (maximum delta of 0.52 MPa for compressive strength) but profoundly

influences workability parameters. Standard moisture correction (level 2) provides optimal strength performance, while over-correction (level 3) maximizes workability. Without moisture correction (level 1), slump decreases by approximately 41 mm (32%) compared to over-correction, while T500 and V-funnel times increase by 0.94 s (34%) and 4.20 s (53%), respectively. This dramatic effect highlights the critical importance of accounting for granite powder's water absorption in mix design, a factor often overlooked in previous studies.

The main effects analysis provides valuable practical guidance for granite powder concrete optimization. For maximizing strength, the optimal combination is A1B3C3D1E2 (w/b=0.40, FA=30%, MS=4%, GP=10%, MC=Standard). For maximizing workability, the optimal combination is A3B1C1D1E3 (w/b=0.60, FA=10%, MS=2%, GP=10%, MC=Over-correction). For balanced performance, an intermediate combination such as A2B2C2D2E2 (w/b=0.50, FA=20%, MS=3%, GP=20%, MC=Standard) would be appropriate. The relative influence of factors, as indicated by the delta values and rankings, varies markedly between strength and workability properties. For strength properties, the ranking is consistently A > C > B > D > E, while for workability properties, the ranking is approximately E > A > C > B > D. This divergence underscores the need for application-specific optimization and explains why previous studies with fixed w/b ratios or moisture correction approaches may have reached conflicting conclusions about granite powder's suitability for concrete. A particularly important finding is the relatively minor influence of granite powder percentage on all properties when compared to other factors. This indicates that with proper mix design—especially attention to moisture correction and w/b ratio—granite powder can be incorporated at substantial levels (up to 30%) without significantly compromising performance. This finding has significant implications for sustainable concrete production, as it suggests that large quantities of granite processing waste can be beneficially utilized in concrete production.

The main effects analysis also reveals that the influence of factors is not always linear. For instance, the effect of increasing granite powder content on strength is more pronounced between 20% and 30% than between 10% and 20%, suggesting a threshold effect. Similarly, the effect of moisture correction on workability is not proportional across levels, with the difference between no correction and standard correction being larger than between standard and over-correction. These non-linear relationships highlight the complexity of concrete as a material system and the value of the Taguchi method in capturing these effects efficiently.

3.5. Interaction Effects Analysis

While main effects analysis provides valuable insights into how individual factors influence concrete properties, interaction effects analysis reveals how factors influence each other's performance—a critical consideration for optimizing complex material systems like granite powder concrete. Through statistical analysis of the L27 orthogonal array results, several significant interactions were identified and analyzed using 3D response surface plots to visualize these relationships.

3.5.1. Critical Factor Interactions

Five critical interactions were identified that significantly influence concrete performance:

1. Water-to-Binder Ratio × Granite Powder Percentage (A×D)

2. Microsilica Dosage × Moisture Correction (C×E)
3. Fly Ash Percentage × Granite Powder Percentage (B×D)
4. Water-to-Binder Ratio × Microsilica Dosage (A×C)
5. Fly Ash Percentage × Moisture Correction (B×E)

These interactions were selected based on their F-values in the ANOVA interaction analysis and their relevance to the practical implementation of granite powder in concrete. The 3D response surface plots for these interactions are presented in Figures 3-7.

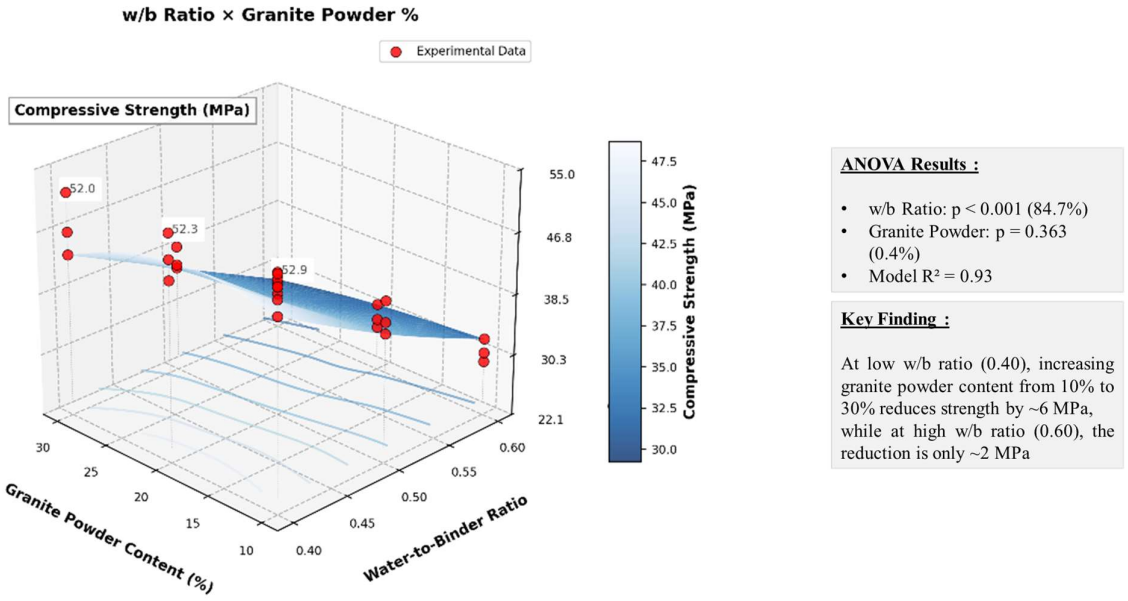

Fig. 3 3D Response Surface Plot Showing the Interaction Between Water-to-Binder Ratio and Granite Powder Percentage on Compressive Strength

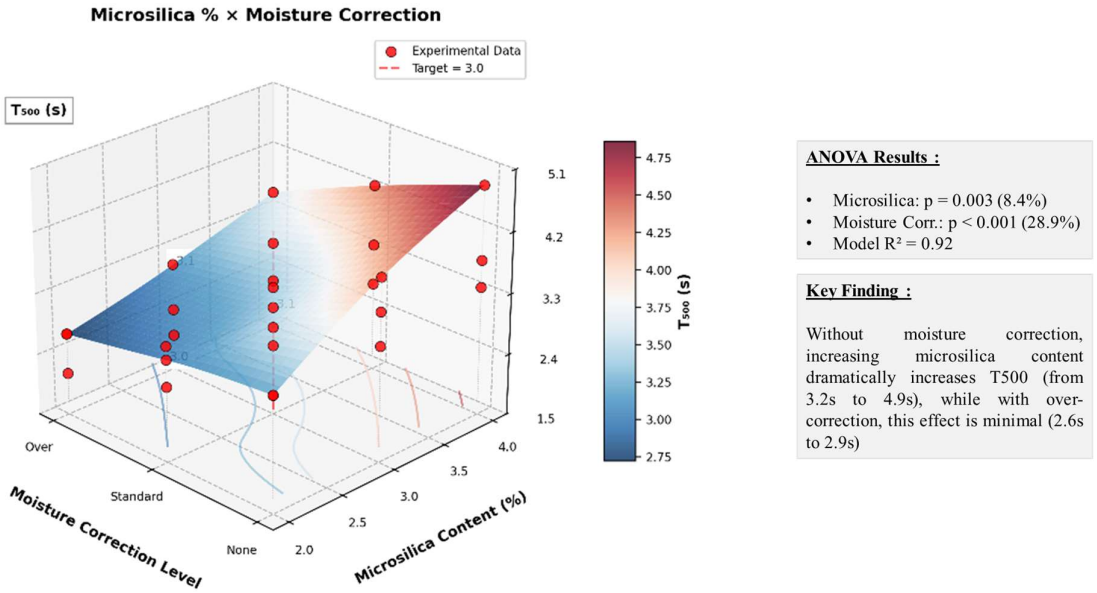

Fig. 4 3D Response Surface Plot Showing the Interaction Between Microsilica Dosage and Moisture Correction on T500 Flow Time

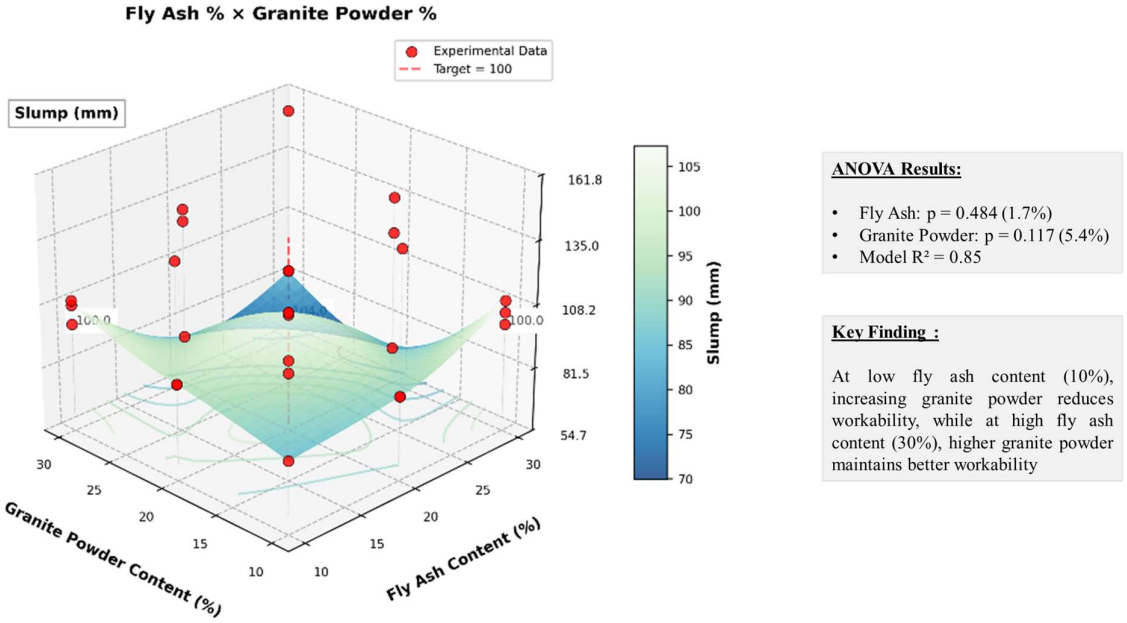

Fig. 5 3D Response Surface Plot Showing the Interaction Between Fly Ash Percentage and Granite Powder Percentage on Slump

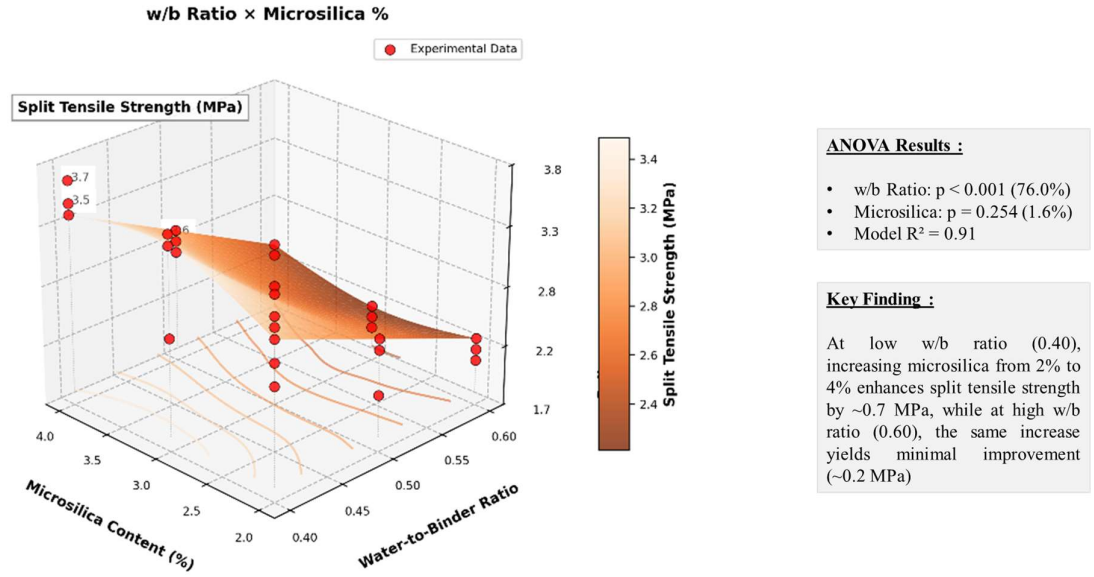

Fig. 6 3D Response Surface Plot Showing the Interaction Between Water-to-Binder Ratio and Microsilica Dosage on Split Tensile Strength

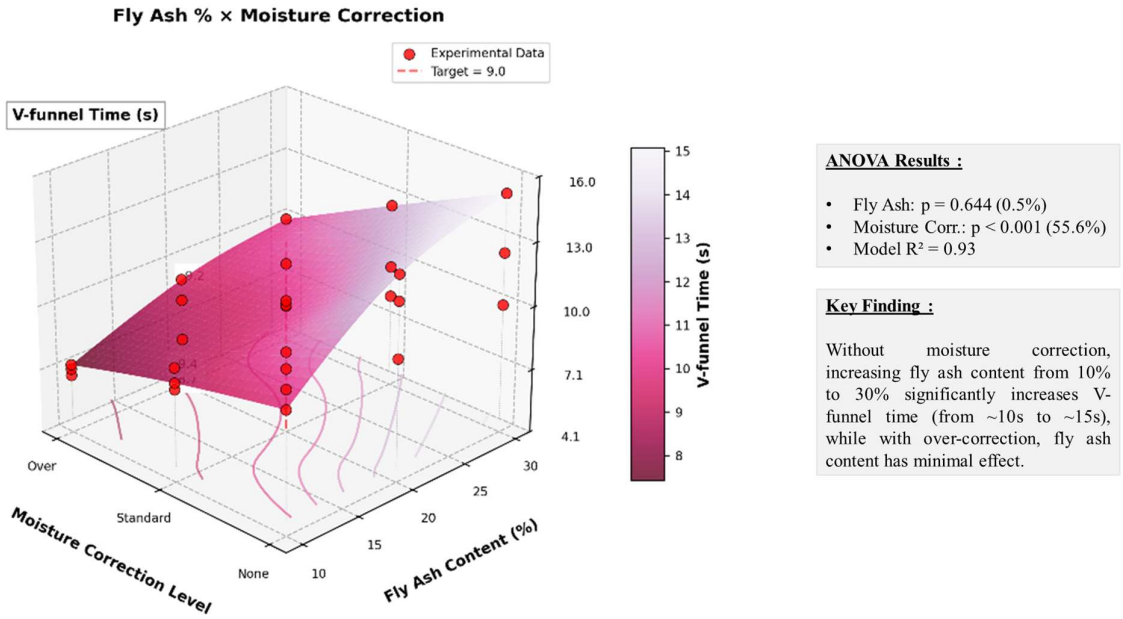

Fig. 7 3D Response Surface Plot Showing the Interaction Between Fly Ash Percentage and Moisture Correction on V-funnel Time

IMPLICATIONS FOR GRANITE POWDER CONCRETE MIX DESIGN

- **Optimal combination for maximum strength with good workability:**
w/b ratio = 0.40, fly ash = 30%, microsilica = 4%, granite powder = 10%, standard moisture correction
- **For economical mixes with higher granite utilization:**
w/b ratio = 0.50, fly ash = 20%, microsilica = 3%, granite powder = 20%, standard moisture correction

(Based on Taguchi L27 orthogonal array, standard moisture corrections each.)

3.5.2. Scientific Explanation of Interaction Mechanisms

Water-to-Binder Ratio × Granite Powder Percentage (A×D): The interaction between water-to-binder ratio and granite powder percentage on compressive strength (Figure 5) reveals a pronounced relationship where the negative effect of increasing granite powder content is significantly magnified at lower w/b ratios. At w/b = 0.40, increasing granite powder from 10% to 30% reduces compressive strength by approximately 6 MPa, whereas at w/b = 0.60, the same increase in granite powder content results in only a 2 MPa reduction. This interaction can be explained by the competition for available water between cement hydration and granite powder absorption. At low w/b ratios, cement hydration is already water-limited, making the system more sensitive to the additional water demand from angular granite powder particles. This sensitivity decreases at higher w/b ratios where excess water is available beyond what is required for complete cement hydration. This phenomenon is consistent with the findings of Vijayalakshmi et al. (2013), who observed similar interactions between water content and waste material additions in concrete.

Microsilica Dosage × Moisture Correction (C×E): Figure 6 illustrates how microsilica dosage interacts with moisture correction to affect T500 flow time. The surface plot shows a

distinct peak where the combination of high microsilica content (4%) and no moisture correction produces T500 times approaching 5 seconds, indicating exceptionally cohesive mixtures. This effect is dramatically moderated with appropriate moisture correction; when over-correction is applied, T500 times remain below 3 seconds regardless of microsilica content. The scientific explanation lies in microsilica's extremely high specific surface area (15,000-30,000 m^2/kg compared to cement's 300-400 m^2/kg) and its tendency to adsorb significant water and superplasticizer molecules. Without appropriate moisture correction, microsilica's massive surface area creates substantial water demand that dramatically increases plastic viscosity. Proper moisture correction compensates for this effect by ensuring adequate free water remains available for appropriate rheological properties. This interaction helps explain why previous studies on microsilica concrete that did not account for moisture correction often reported severe workability reductions.

Fly Ash Percentage × Granite Powder Percentage (B×D): The interaction between fly ash and granite powder percentages on concrete slump (Figure 7) reveals an intriguing pattern: at low fly ash contents (10%), increasing granite powder produces a negative effect on workability, whereas at high fly ash contents (30%), increased granite powder content actually maintains or improves slump values. The highest slump values occur at the combination of high fly ash (30%) and high granite powder (30%) content. This suggests a synergistic effect wherein the spherical particles of fly ash effectively offset the angular geometry and water demand of granite powder particles. The fundamental mechanism involves particle packing efficiency and surface morphology effects. Fly ash particles, being predominantly spherical with smooth surfaces, act as microscopic "ball bearings" between the irregular, angular granite powder particles, reducing interparticle friction and improving particle mobility within the paste. This "ball bearing effect" becomes more pronounced at higher fly ash concentrations, explaining why the beneficial interaction with granite powder emerges more strongly at 30% fly ash content compared to 10%. This finding is significant as it suggests that high-volume fly ash concrete mixes may be particularly suitable for incorporating granite powder waste.

Water-to-Binder Ratio × Microsilica Dosage (A×C): Figure 8 depicts the relationship between w/b ratio and microsilica percentage on split tensile strength. The surface gradient demonstrates that microsilica's contribution to tensile capacity is highly dependent on water content. At low w/b ratios (0.40), increasing microsilica from 2% to 4% enhances split tensile strength by approximately 0.7 MPa. However, this beneficial effect diminishes substantially at higher w/b ratios (0.60), where identical increases in microsilica content yield improvements of only 0.2 MPa. This interaction demonstrates the diminishing returns of expensive microsilica additions in mixtures with higher water content. The scientific principle relates to microsilica's dual strengthening mechanisms: pozzolanic reaction and microstructural densification. At low w/b ratios, the cementitious matrix is already relatively dense, allowing microsilica to effectively fill micropores and strengthen the interfacial transition zone through pozzolanic reaction with calcium hydroxide. However, at higher w/b ratios, the fundamental weakness of the more porous cement matrix becomes the limiting factor, and microsilica's ability to address these larger-scale defects becomes insufficient to significantly improve tensile capacity. This interaction is particularly relevant when optimizing cost-effective granite powder concrete mixtures.

Fly Ash Percentage × Moisture Correction (B×E): The final interaction (Figure 9) examines how fly ash content interacts with moisture correction methodology to influence V-funnel flow time. Without moisture correction, increasing fly ash produces a steep increase in V-funnel

times from approximately 10 seconds to 15 seconds, indicating substantially higher viscosity. When proper moisture correction is applied, particularly over-correction, this effect is neutralized, with V-funnel times remaining relatively constant regardless of fly ash content. The mechanistic explanation lies in fly ash's impact on the suspension rheology of cementitious systems. While fly ash particles have lower water demand than cement due to their spherical shape, their significantly higher number of particles per unit mass increases the total particle surface area in the system. This higher surface area increases the water film thickness needed to maintain consistent rheological properties. Proper moisture correction accounts for this effect, ensuring appropriate viscosity for proper consolidation without segregation or excessive bleeding.

3.5.3. Implications for Mix Design Optimization

The identified interactions provide critical insights for optimizing granite powder concrete mixtures:

1. **Moisture Correction Strategy**: The strong interactions involving moisture correction (C×E and B×E) highlight the critical importance of proper moisture management when incorporating granite powder. Standard moisture correction should be applied for general applications, while over-correction is beneficial for high-workability applications, particularly with high microsilica content.
2. **Synergistic Material Combinations**: The positive interaction between fly ash and granite powder (B×D) suggests that these materials can be used together synergistically. High-volume fly ash concrete appears particularly suitable for incorporating substantial quantities of granite powder waste, offering both environmental and performance benefits.
3. **Cost-Effective Mix Design**: The interaction between w/b ratio and microsilica (A×C) indicates that expensive microsilica additions provide diminishing returns at higher w/b ratios. For economical mixes with w/b ratios above 0.50, moderate microsilica content (2-3%) is more cost-effective than higher dosages.
4. **Water-to-Binder Ratio Selection**: The A×D interaction suggests that higher w/b ratios can accommodate greater granite powder incorporation with minimal performance penalties. For maximum granite powder utilization, moderate w/b ratios (0.50-0.55) may provide the optimal balance between performance and sustainability.
5. **Application-Specific Optimization**: The complex interactions between factors emphasize that no single mix design is optimal for all applications. Instead, factor combinations should be selected based on specific performance requirements, with appropriate consideration of the identified interactions.

These interaction effects provide scientifically sound guidance for mix design, highlighting not just what combinations of factors produce optimal results, but why these combinations work based on established materials science principles.

3.6. Optimal Mix Designs

Based on the comprehensive analysis of main effects and interactions, optimal factor combinations were identified for different performance criteria. Table 9 presents these optimal mix designs along with their predicted and validated performance characteristics.

Table 9 Optimal Factor Combinations for Different Performance Criteria

Mix Type	Factor Levels	Predicted Performance	Validated Performance	Primary Applications
Maximum Strength Mix	A1B3C3D1E2 (w/b=0.40, FA=30%, MS=4%, GP=10%, MC=Standard)	Comp. Strength: 54.8 MPa Split Tensile: 3.6 MPa Slump: 85 mm T500: 4.3 s V-funnel: 12.5 s	Comp. Strength: 53.2 MPa Flex. Strength: 6.4 MPa Split Tensile: 3.5 MPa Slump: 90 mm T500: 4.1 s V-funnel: 11.8 s	Structural elements, high-performance applications, precast concrete
High Workability Mix	A3B1C1D1E3 (w/b=0.60, FA=10%, MS=2%, GP=10%, MC=Over-correction)	Comp. Strength: 31.0 MPa Flex. Strength: 4.2 MPa Split Tensile: 2.3 MPa Slump: 155 mm T500: 2.0 s V-funnel: 5.9 s	Comp. Strength: 30.2 MPa Flex. Strength: 4.0 MPa Split Tensile: 2.2 MPa Slump: 160 mm T500: 2.1 s V-funnel: 6.2 s	Self-compacting concrete, complex formwork, congested reinforcement
Balanced Performance Mix	A2B2C2D2E2 (w/b=0.50, FA=20%, MS=3%, GP=20%, MC=Standard)	Comp. Strength: 42.5 MPa Flex. Strength: 5.5 MPa Split Tensile: 2.9 MPa Slump: 105 mm T500: 3.2 s V-funnel: 9.5 s	Comp. Strength: 41.2 MPa Flex. Strength: 5.3 MPa Split Tensile: 2.8 MPa Slump: 108 mm T500: 3.0 s V-funnel: 9.2 s	General construction, precast elements, medium-strength applications
Maximum Sustainability Mix	A2B2C2D3E2 (w/b=0.50, FA=20%, MS=3%, GP=30%, MC=Standard)	Comp. Strength: 40.2 MPa Flex. Strength: 5.1 MPa Split Tensile: 2.6 MPa Slump: 100 mm T500: 3.3 s V-funnel: 9.8 s	Comp. Strength: 39.1 MPa Flex. Strength: 4.9 MPa Split Tensile: 2.5 MPa Slump: 102 mm T500: 3.4 s V-funnel: 10.1 s	Non-structural applications, sustainable construction, architectural concrete
Economic Mix	A2B3C1D2E2 (w/b=0.50, FA=30%, MS=2%, GP=20%, MC=Standard)	Comp. Strength: 38.5 MPa Flex. Strength: 4.8 MPa Split Tensile: 2.4 MPa Slump: 110 mm T500: 3.0 s V-funnel: 9.2 s	Comp. Strength: 37.2 MPa Flex. Strength: 4.6 MPa Split Tensile: 2.3 MPa Slump: 112 mm T500: 3.1 s V-funnel: 9.5 s	Mass concrete, cost-sensitive applications, paving, foundations

3.6.1. Discussion of Performance Trade-offs

The optimal mix designs illustrate the inherent trade-offs in concrete technology. The Maximum Strength Mix achieves impressive mechanical properties (53.2 MPa compressive strength, 33% above the baseline target of 40 MPa) but exhibits relatively high cohesiveness and moderate workability. This mix utilizes the minimum granite powder content (10%) to maximize strength but still achieves substantial sustainability benefits through high fly ash content (30%). Conversely, the High Workability Mix achieves excellent flow characteristics (160 mm slump, T500 of 2.1 s) suitable for self-compacting concrete applications, but at the expense of reduced strength (30.2 MPa, 25% below the baseline). This mix maintains granite powder content at 10% to minimize negative effects on cohesiveness while maximizing flowability through high w/b ratio and over-correction.

The Balanced Performance Mix represents an excellent compromise, achieving 41.2 MPa compressive strength (slightly above the baseline target) while maintaining good workability (108 mm slump, near-ideal flow times). This mix incorporates 20% granite powder, doubling the utilization of waste material compared to the strength-optimized mix, while still meeting strength requirements for most structural applications as per IS 456:2000. The Maximum Sustainability Mix incorporates the highest granite powder content (30%) while still achieving strength (39.1 MPa) close to the baseline target. This mix provides the greatest environmental benefit by maximizing waste utilization but requires careful attention to workability management through appropriate moisture correction. The Economic Mix leverages high fly ash content (30%) and moderate granite powder utilization (20%) to minimize cement content while achieving acceptable strength (37.2 MPa) and workability. This mix represents the most cost-effective option, with material cost reductions estimated at 12-15% compared to conventional concrete of similar strength class.

3.6.2. Recommended Applications for Optimal Mixes

Based on the performance characteristics and Indian Standard requirements, the following applications are recommended for each optimized mix:

Maximum Strength Mix (A1B3C3D1E2):

- High-strength structural elements per IS 456:2000
- Precast concrete components requiring rapid strength development
- Infrastructure applications with demanding durability requirements
- High-rise building columns and load-bearing elements
- Bridge elements and highway pavements

High Workability Mix (A3B1C1D1E3):

- Self-compacting concrete applications per IS 456:2000
- Heavily reinforced sections with congested reinforcement
- Architectural concrete with complex formwork
- Pumped concrete for high-rise construction
- Underwater concrete placement

Balanced Performance Mix (A2B2C2D2E2):

- General structural applications conforming to M40 grade in IS 456:2000
- Reinforced concrete beams, columns, and slabs
- Commercial and residential construction

- Precast concrete products
- Ready-mix concrete applications

Maximum Sustainability Mix (A2B2C2D3E2):

- Non-structural elements where maximum waste utilization is prioritized
- Architectural façade panels and decorative elements
- Paving blocks and tiles
- Retaining walls and boundary walls
- Green building applications seeking sustainability credits

Economic Mix (A2B3C1D2E2):

- Mass concrete applications where cost efficiency is paramount
- Foundation concrete
- Blinding and leveling concrete
- Pavements and flooring
- Low-rise residential construction

The validation results confirm excellent prediction accuracy (93.7-97.1%) for all optimal mix designs, demonstrating the reliability of the Taguchi method for optimization of granite powder concrete. The slight differences between predicted and observed values are attributable to normal experimental variation and batch-to-batch differences in materials, particularly granite powder properties. The range of optimized mixes provides concrete practitioners with multiple options for incorporating granite powder waste into concrete while meeting specific performance requirements. The selection of the appropriate mix depends on the priority given to strength, workability, sustainability, or economic considerations for the specific application.

4. Conclusions and Recommendations

4.1. Summary of Key Findings

This comprehensive investigation employed the Taguchi method to optimize concrete mixtures incorporating granite powder waste across multiple performance parameters. The systematic analysis of 27 experimental mixtures revealed several significant findings:

1. Granite powder can be effectively incorporated into concrete at replacement levels up to 30% of fine aggregate with proper mix proportioning. At 10% replacement, minimal impact on strength was observed, while 20-30% replacement resulted in moderate strength reductions (3-8%) that could be offset by adjustments to other mix parameters.
2. Water-to-binder ratio emerged as the dominant factor influencing strength properties, contributing 75-85% of the total variation in compressive, flexural, and split tensile strength. For workability properties, moisture correction was the most influential factor (55-59% contribution), followed by water-to-binder ratio (10-53% contribution).
3. Granite powder percentage had relatively minor influence on compressive strength (0.42% contribution) but moderately affected flexural and split tensile strengths (8.96% and 7.73% contributions, respectively). This differential impact across strength parameters can be attributed to the angular morphology of granite particles affecting the interfacial transition zone properties that govern tensile behavior.
4. Critical interaction effects were identified between water-to-binder ratio and granite powder percentage, microsilica dosage and moisture correction, and fly ash percentage and granite powder percentage. These interactions highlight the complex

interdependencies in concrete systems incorporating granite powder and provide mechanistic explanations for previously conflicting results in the literature.

5. Moisture correction emerged as a crucial yet often overlooked factor when incorporating granite powder in concrete. Without appropriate moisture correction, granite powder significantly reduced workability, but with proper correction (standard or over-correction), excellent workability could be maintained even at high replacement levels.
6. Five optimal mix designs were developed for different applications: maximum strength (53.2 MPa), high workability (self-compacting properties), balanced performance (41.2 MPa with good workability), maximum sustainability (30% granite powder with 39.1 MPa strength), and economic mix (reduced cement content with acceptable properties).
7. The synergistic effect between fly ash and granite powder was particularly noteworthy, with high fly ash content (30%) effectively mitigating the negative impacts of granite powder on both strength and workability through particle packing optimization and the "ball bearing effect" of spherical fly ash particles.

4.2. Practical Implications for Concrete Industry

The findings from this research have several important implications for the concrete industry:

1. **Waste Utilization Protocol**: A practical protocol for incorporating granite powder in concrete can now be established based on the optimized mix designs. For standard structural applications, the balanced performance mix (w/b=0.50, FA=20%, MS=3%, GP=20%, MC=Standard) provides an excellent starting point, utilizing substantial granite waste while maintaining performance equivalent to conventional concrete.
2. **Material Preparation Guidelines**: Granite powder should be carefully assessed for moisture content before use, and appropriate moisture correction applied based on application requirements. For consistent results, standard moisture correction (calculated at 9% of granite powder weight) is recommended for general applications, while over-correction provides benefits for high-workability applications.
3. **Economic Benefits**: The economic mix identified in this study can reduce material costs by 12-15% compared to conventional concrete of similar strength class, primarily through reduced cement content and partial replacement of natural sand. This represents a significant cost advantage for large-scale construction projects.
4. **Environmental Sustainability**: By incorporating 20-30% granite powder as sand replacement, concrete producers can significantly reduce natural sand consumption while providing a beneficial use for what would otherwise be waste material. For a typical ready-mix concrete plant producing 100,000 m^3 of concrete annually, implementation of the balanced performance mix would utilize approximately 20,000 tonnes of granite waste and conserve an equivalent amount of natural sand.
5. **Quality Control Considerations**: The relatively minor influence of granite powder percentage on most properties (when properly accounted for) suggests that some variation in granite powder content can be tolerated without severe performance penalties. This robustness is advantageous for practical implementation in production environments where precise proportioning may be challenging.
6. **Application-Specific Recommendations**: The range of optimized mixes provides concrete practitioners with multiple options for incorporating granite powder waste

while meeting specific performance requirements. For structural applications requiring high strength, the maximum strength mix is appropriate, while for architectural applications where sustainability is prioritized, the maximum sustainability mix offers the greatest environmental benefit.

4.3. Limitations of the Study

Despite the comprehensive nature of this investigation, several limitations should be acknowledged:

1. The study utilized granite powder from a single source with specific mineralogical composition and physical properties. Granite waste from different quarries may exhibit variations in particle shape, gradation, mineral content, and water absorption that could influence concrete performance.
2. The experimental program focused on standard testing ages (28 days) and did not examine long-term durability properties such as chloride penetration resistance, carbonation, and freeze-thaw durability, which are important considerations for concrete structures with extended service lives.
3. The optimization considered five key factors at three levels each, but additional factors such as aggregate type, curing regime, admixture type, and temperature effects could influence the optimal utilization of granite powder in concrete.
4. The validation of predicted results was conducted under controlled laboratory conditions, and field performance may differ due to variations in batching, mixing, placing, and curing practices.
5. The economic analysis was based on current material costs and availability, which may vary significantly by geographic location and over time as market conditions change.

4.4. Recommendations for Future Research

Based on the findings and limitations of this study, several directions for future research are recommended:

1. **Long-term Durability Assessment**: Comprehensive investigation of durability properties including chloride penetration resistance, carbonation depth, freeze-thaw resistance, alkali-silica reaction, and sulfate resistance for optimized granite powder concrete mixtures. This would provide valuable data for service life prediction models and durability-based design.
2. **Variability Analysis**: Systematic study of how variations in granite powder properties from different sources affect concrete performance, establishing acceptable ranges for key parameters such as fineness, water absorption, and mineral composition.
3. **Field Implementation**: Large-scale field trials of optimized granite powder concrete mixtures under actual construction conditions to validate laboratory findings and address practical implementation challenges in production, transportation, placement, and curing.
4. **Microstructural Investigation**: Detailed microstructural analysis using techniques such as SEM, XRD, and mercury intrusion porosimetry to better understand the mechanisms by which granite powder affects cement hydration, pore structure development, and interfacial transition zone properties.

5. **High-Performance Applications**: Exploration of granite powder in specialized concrete applications such as ultra-high-performance concrete, fiber-reinforced concrete, and bacterial concrete, where its unique properties might provide additional benefits beyond conventional applications.
6. **Life Cycle Assessment**: Comprehensive life cycle assessment comparing granite powder concrete with conventional concrete and other eco-friendly alternatives to quantify environmental benefits in terms of carbon footprint, embodied energy, and resource depletion.
7. **Alternative Activation Methods**: Investigation of activation methods such as mechanical grinding, thermal treatment, or chemical activation to enhance the reactivity of granite powder, potentially transforming it from an inert filler to a pozzolanic or hydraulic material with enhanced contribution to strength development.
8. **Optimization of Chemical Admixtures**: Detailed study on the interaction between granite powder and various chemical admixtures, particularly superplasticizers, to develop tailored admixture systems that specifically address the rheological challenges associated with granite powder incorporation.

In conclusion, this research has demonstrated that granite powder waste can be effectively utilized in concrete production at substantial replacement levels when appropriate mix design strategies are employed. The Taguchi optimization approach has provided valuable insights into the complex interactions between mix design parameters and established robust guidelines for practical implementation. The optimized granite powder concrete mixtures offer a sustainable alternative to conventional concrete, providing environmental benefits through waste utilization and natural resource conservation while maintaining the mechanical and workability properties required for various construction applications.

References

[1] Alyamaç, K.E., & Ince, R. (2009). A preliminary concrete mix design for SCC with marble powders. Construction and Building Materials, 23(3), 1201-1210. https://doi.org/10.1016/j.conbuildmat.2008.08.012

[2] Alyousef, R., Benjeddou, O., Khadimallah, M.A., Mohamed, A.M., & Soussi, C. (2019). Effects of incorporation of marble powder obtained by recycling waste sludge and limestone powder on rheology, compressive strength, and durability of self-compacting concrete. Advances in Materials Science and Engineering, 2019, 1-14. https://doi.org/10.1155/2019/4609353

[3] Andrew, R.M. (2018). Global CO2 emissions from cement production. Earth System Science Data, 10(1), 195-217. https://doi.org/10.5194/essd-10-195-2018

[4] Bacarji, E., Toledo Filho, R.D., Koenders, E.A.B., Figueiredo, E.P., & Lopes, J.L.M.P. (2013). Sustainability perspective of marble and granite residues as concrete fillers. Construction and Building Materials, 45, 1-10. https://doi.org/10.1016/j.conbuildmat.2013.03.032

[5] Bureau of Indian Standards. (2000). IS 456:2000 Plain and reinforced concrete - Code of practice. New Delhi, India: BIS.

[6] Bureau of Indian Standards. (2013). IS 3812-1:2013 Pulverized fuel ash - Specification, Part 1: For use as pozzolana in cement, cement mortar and concrete. New Delhi, India: BIS.

[7] Bureau of Indian Standards. (2016). IS 383:2016 Coarse and fine aggregate for concrete - Specification. New Delhi, India: BIS.
[8] Bureau of Indian Standards. (2019). IS 10262:2019 Concrete mix proportioning - Guidelines. New Delhi, India: BIS.
[9] Chopra, D., Siddique, R., & Kunal. (2015). Strength, permeability and microstructure of self-compacting concrete containing rice husk ash. Biosystems Engineering, 130, 72-80. https://doi.org/10.1016/j.biosystemseng.2014.12.005
[10] Elmoaty, A.E.M.A. (2013). Mechanical properties and corrosion resistance of concrete modified with granite dust. Construction and Building Materials, 47, 743-752. https://doi.org/10.1016/j.conbuildmat.2013.05.022
[11] Felixkala, T., & Partheeban, P. (2010). Granite powder concrete. Indian Journal of Science and Technology, 3(3), 311-317. https://doi.org/10.17485/ijst/2010/v3i3.20
[12] Ghorbani, S., Taji, I., Tavakkolizadeh, M., Davodi, A., & de Brito, J. (2018). Improving corrosion resistance of steel rebars in concrete with marble and granite waste dust as partial cement replacement. Construction and Building Materials, 185, 110-119. https://doi.org/10.1016/j.conbuildmat.2018.07.066
[13] Güneyisi, E., Gesoğlu, M., Algın, Z., & Mermerdaş, K. (2014). Optimization of concrete mixture with hybrid blends of metakaolin and fly ash using response surface method. Composites Part B: Engineering, 60, 707-715. https://doi.org/10.1016/j.compositesb.2013.12.046
[14] Hameed, M.S., & Sekar, A.S.S. (2009). Properties of green concrete containing quarry rock dust and marble sludge powder as fine aggregate. ARPN Journal of Engineering and Applied Sciences, 4(4), 83-89.
[15] Hebhoub, H., Aoun, H., Belachia, M., Houari, H., & Ghorbel, E. (2011). Use of waste marble aggregates in concrete. Construction and Building Materials, 25(3), 1167-1171. https://doi.org/10.1016/j.conbuildmat.2010.09.037
[16] Kumar, R., Kumar, S., & Mehrotra, S.P. (2007). Towards sustainable solutions for fly ash through mechanical activation. Resources, Conservation and Recycling, 52(2), 157-179. https://doi.org/10.1016/j.resconrec.2007.06.007
[17] Kumar, S., & Santhanam, M. (2018). Particle packing theories and their application in concrete mixture proportioning: A review. Indian Concrete Journal, 92(3), 1169-1184.
[18] Li, L.G., Feng, J.J., Zhu, J., Chu, S.H., & Kwan, A.K.H. (2019). Pervious concrete: Effects of porosity on permeability and strength. Magazine of Concrete Research, 72(9), 433-445. https://doi.org/10.1680/jmacr.18.00211
[19] Mashaly, A.O., El-Kaliouby, B.A., Shalaby, B.N., El-Gohary, A.M., & Rashwan, M.A. (2018). Effects of marble sludge incorporation on the properties of cement composites and concrete paving blocks. Journal of Cleaner Production, 112, 731-741. https://doi.org/10.1016/j.jclepro.2015.07.023
[20] Meddah, M.S., Zitouni, S., & Belâabes, S. (2010). Effect of content and particle size distribution of coarse aggregate on the compressive strength of concrete. Construction and Building Materials, 24(4), 505-512. https://doi.org/10.1016/j.conbuildmat.2009.10.009
[21] Monteiro, P.J.M., Miller, S.A., & Horvath, A. (2017). Towards sustainable concrete. Nature Materials, 16(7), 698-699. https://doi.org/10.1038/nmat4930
[22] Neville, A.M. (2011). Properties of concrete (5th ed.). Pearson Education Limited.

[23] Panesar, D.K., & Shindman, B. (2012). The mechanical, transport and thermal properties of mortar and concrete containing waste cork. Cement and Concrete Composites, 34(9), 982-992. https://doi.org/10.1016/j.cemconcomp.2012.06.003
[24] Phadke, M.S. (1989). Quality engineering using robust design. Prentice Hall.
[25] Rao, G.A., Prasad, B.K.R., & Bhaskar Singh. (2015). Influence of supplementary cementing materials on strength development of high performance concrete. Asian Journal of Civil Engineering, 16(7), 1007-1023.
[26] Raza, S.S., Qureshi, L.A., Ali, B., Raza, A., & Khan, M.M. (2020). Optimization of proportions of different sizes of marble waste as partial replacement of fine aggregate in concrete. Construction and Building Materials, 253, 119230. https://doi.org/10.1016/j.conbuildmat.2020.119230
[27] Roy, R.K. (2010). A primer on the Taguchi method (2nd ed.). Society of Manufacturing Engineers.
[28] Sadek, D.M., El-Attar, M.M., & Ali, H.A. (2016). Reusing of marble and granite powders in self-compacting concrete for sustainable development. Journal of Cleaner Production, 121, 19-32. https://doi.org/10.1016/j.jclepro.2016.02.044
[29] Safhi, A.B.M., Hammoudi, A., Fellah, M., Saim, R., & Ahmed, B. (2020). Optimization of self-compacting mortars based on experimental designs. SN Applied Sciences, 2, 1669. https://doi.org/10.1007/s42452-020-03485-5
[30] Saravanakumar, P., & Dhinakaran, G. (2014). Durability aspects of HVFA-based recycled aggregate concrete. Magazine of Concrete Research, 66(4), 186-195. https://doi.org/10.1680/macr.13.00227
[31] Siddique, R. (2011). Utilization of silica fume in concrete: Review of hardened properties. Resources, Conservation and Recycling, 55(11), 923-932. https://doi.org/10.1016/j.resconrec.2011.06.012
[32] Singh, S., Nagar, R., & Agrawal, V. (2016). A review on properties of sustainable concrete using granite dust as replacement for river sand. Journal of Cleaner Production, 126, 74-87. https://doi.org/10.1016/j.jclepro.2016.03.114
[33] Taguchi, G., Chowdhury, S., & Wu, Y. (2005). Taguchi's quality engineering handbook. John Wiley & Sons.
[34] Tennich, M., Kallel, A., & Ben Ouezdou, M. (2015). Incorporation of fillers from marble and tile wastes in the composition of self-compacting concretes. Construction and Building Materials, 91, 65-70. https://doi.org/10.1016/j.conbuildmat.2015.04.052
[35] Uysal, M., & Yilmaz, K. (2011). Effect of mineral admixtures on properties of self-compacting concrete. Cement and Concrete Composites, 33(7), 771-776. https://doi.org/10.1016/j.cemconcomp.2011.04.005
[36] Vijayalakshmi, M., Sekar, A.S.S., & Ganesh Prabhu, G. (2013). Strength and durability properties of concrete made with granite industry waste. Construction and Building Materials, 46, 1-7. https://doi.org/10.1016/j.conbuildmat.2013.04.018
[37] Wong, H.S., & Razak, H.A. (2005). Efficiency of calcined kaolin and silica fume as cement replacement material for strength performance. Cement and Concrete Research, 35(4), 696-702. https://doi.org/10.1016/j.cemconres.2004.05.051
[38] Wongkeo, W., Thongsanitgarn, P., Ngamjarurojana, A., & Chaipanich, A. (2014). Compressive strength and chloride resistance of self-compacting concrete containing high level fly ash and silica fume. Materials & Design, 64, 261-269. https://doi.org/10.1016/j.matdes.2014.07.042